TH-AM-1 UNCLOCKLIKE BEHAVIOR OF A BIOLOGICAL CLOCK
A.T. Winfree, Dept. of Biol. Sci., Purdue University, W. Lafayette, Ind.

In the fruitfly Drosophila, a circadian oscillation which begins in the youngest larva eventually determines the time of pupal eclosion and the emerged adult's daily activity rhythm. Though its cellular mechanism remains undiscovered, it is believed to be either a clock-like process in which all possible states are repeatedly traversed in cyclic order, or a limit cycle process in which there exist accessible states off the asymptotic cycle (e.g. an equilibrium point) but recovery from most such states to normal cycling takes only minutes or hours.
Both assumptions, though stated in qualitative terms, have quantitative implications for the measurable dependence of new phase on the timing and intensity of a phase-resetting disturbance, e.g. exposure to blue light. Our experimental results indicate that neither assumption is correct. In contrast, it appears that blue light simultaneously resets both the phase and the amplitude of the circadian oscillation in the coordinated way characteristic of orbitally stable oscillations (such as a pendulum).
If this seems an unappealing spectre, there is an alternative interpretation: The organism's behavioral rhythm might be determined collectively by a number of independent, autonomous circadian clocks of almost any kind. If such a population were imperfectly coherent, then its pattern of phase and (collective) amplitude lability would resemble the experimental response of Drosophila's clock, with the organism's phase determined by the mean phase of its cellular clocks and its amplitude determined by the variance of cellular phases.

TH-AM-2 THE MITOTIC OSCILLATOR IN PHYSARUM POLYCEPHALUM II, S.A. Kauffman*
J.J. Wille*, Lab. of Theoretical Biology, NCI, NIH, Bethesda, MD 20014., Dept. of Biophysics & Theoretical Biology, Univ. of Chicago, Chi., IL60637

Previous theories of the mitotic clock are: a closed causal loop of discrete events of the cycle; increase in concentration of a division protein to a threshold which triggers mitosis and causes division protein to fall to a low initial level. We propose that the mitotic clock is a sustained biochemical oscillation in a non-linear dynamical system. This model predicts that short heat shocks soon after mitosis should phase advance the next mitosis, then as G2 advances, short shocks should yield a mitotic delay reaching a peak in late G2, and declining to nothing. As heat shock duration in late G2 increases, mitotic delay should jump discontinuously from slight delay, to a full cycle delay, to two full cycles delay, then should decrease to about a half cycle delay for very long heat shocks. Similar shocks in early G2 should yield a monotonic increase in delay, but never more than one cycle delay, with shock duration. After a short late G2 shock delays the first mitosis the second should "catch up". In fusions of two internally synchronous plasmodia at all possible phases and phase differences, a discontinuous jump in mitotic delay of one plasmodium should occur as phase difference increases for a particular phase before mitosis. Fusions at appropriate phases should suppress mitosis in both partners for several cycles. Preliminary evidence supports the last prediction. The rest have been confirmed. A new proceedure, the Arc Discontinuity allows characterization of the waveform of the mitotic clock in Physarum. It is a moderate relaxation oscillation. On this model, cell cell interaction is partially due to coupled oscillations. Bifurcations as diffusion coefficients and other parameters change can lead from a system which synchronizes on fusion, to one which stops cycling.

TH-AM-3 BOX DIFFUSION MODELS OF CHEMICAL ORGANIZATION. J.J. Tyson*, Department of Mathematics and the Center for Theoretical Biology, State University of New York at Buffalo, Buffalo, New York 14221.

When two macroplasmodia of Physarum polycephalum at different phases in the cell cycle are fused, the pair achieves mitotic synchrony after a period of transiency. Kauffman, Wille and Tyson have investigated a box diffusion model of this phenomenon to interpret the results of many experimental fusions. The success of this model provides further justification for the hypothesis that mitosis in this organism is controlled by a continuous cytoplasmic biochemical oscillator. Besides phase synchronization such oscillators, when coupled by diffusion in this manner, exhibit other modes of temporal and spatial organization including: frequency synchronization, generation of oscillations from quiescence, travelling waves, extinction of oscillations and inhomogeneous steady states.

TH-AM-4 A MEMBRANE MODEL FOR THE CIRCADIAN CLOCK. David Njus, The Biological Laboratories, Harvard University, Cambridge, MA 02138.

It has been known for many years that circadian rhythms are exhibited by single isolated cells, so a biological clock mechanism must be sought on a cellular level. We assume that the clock is confined to some specific part of cellular metabolism and that the mechanism for circadian timekeeping is universal. Data from a wide variety of organisms are consistent with these assumptions. Two other generalizations concerning the mechanism of the clock are emerging. First, agents which affect cellular ion concentrations seem to affect circadian timekeeping whereas inhibitors of macromolecular synthesis do not. Second, the phase shifting action of light seems to indicate that the clock is a feedback oscillator rather than a programmed sequence of events. This is all consistent with a membrane model for the circadian clock. Self-sustained oscillations are generated by a feedback system comprised of ions and membrane-bound ion transport systems. According to this model, light acts on the clock either directly or via hormonal coupling to change trans-membrane ion gradients. Phase shifting by light is a consequence of this. Temperature compensation of the free-running period is a consequence, at least in part, of the temperature adaptation of membrane lipids. That is, the kinetics of the clock depend on the homeostatically controlled fluidity of biological membranes. Oscillating ion concentrations control the expression of observed rhythmic phenomena such as photosynthesis, respiration, activity, etc. This model accounts qualitatively for many of the characteristic features of circadian rhythms. This research was supported by NIH grant GM 19536.

TH-POS-C1 GENE DUPLICATIONS IN THE EVOLUTION OF MUSCLE PROTEINS
W. C. Barker and M. O. Dayhoff, National Biomedical Research Foundation, Georgetown Univ. Med. Cen., 3900 Reservoir Road, Washington, D.C. 20007

We have analyzed by computer the sequences of troponin C and myosin A2 light chain from rabbit skeletal muscle and of parvalbumins from fish and frog muscle in order to elucidate their evolutionary history. All of these related proteins show evidence of internal gene duplications. The myosin A2 chain can be aligned with troponin C so that 30% of the residues are identical. The divergence of troponin C and the myosin light chain occurred after two internal duplications had produced a chain four times the length of a common ancestral chain. The duplication that produced a gene for parvalbumin occurred close to that giving rise to separate troponin C and myosin light chains and probably followed the two elongation events. The similarity of the C-terminal 2/3 of parvalbumin to the C-terminal half of troponin C indicates that parvalbumin diverged from the troponin C branch and subsequently lost about 40 residues from its amino end. Since these divergences, the rate of change of troponin C has been about half that of the other two proteins. We calculate that the C-terminal regions of frog and hake parvalbumins are changing at a rate of 4 accepted point mutations per 100 million years. If the rate has been constant, the divergence of parvalbumin, troponin C and myosin light chains occurred over 2 billion years ago, long enough to account for the presence of these proteins in all eukaryote cells. The myosin A1 chain is of recent origin as it is less than 4% different from the A2 chain, except for an amino-terminal 41-residue segment of unusual composition. The DNA coding for this segment probably originated from an intercistronic region high in guanine and low in adenine. *This work was supported by NIH Grant GM 08710.*

TH-POS-C2 CHOLINERGIC RECEPTOR ACTIVATION AND INACTIVATION IN THE ABSENCE OF DEPOLARIZATION. E. G. Henderson, Department of Pharmacology, University of Connecticut Health Center, Farmington, Connecticut 06032.

Cholinomimetic agents did not depolarize the post-junctional membrane of frog sartorius muscle, bathed in Na^+-free solutions, but did cause receptor desensitization (Volle and Reynolds, N.-Schmied. Arch. Pharmacol. 276:49-54, 1973). In the present study it was found that carbamycholine chloride (CARB) (0.05mM) caused a transient 2-3 fold increase in ^{42}K-efflux from denervated (4-8 weeks) frog sartorius muscles bathed in Na^+-free solutions; no change in E_m occurred. The time course of the CARB stimulated ^{42}K-efflux and reversal in Na^+-free solutions was identical with that demonstrated for the depolarization-repolarization sequence in Na^+-containing solutions. The CARB (0.05mM) stimulated ^{42}K-efflux was completely blocked by d-tubocurarine (d-TC) (0.03mM) and the block was completely reversed by washing for 1-hr. in the solution free of d-TC and Na^+. During the exposure to CARB, ^{42}K-efflux stimulation was desensitized to subsequent additions of CARB. Essentially full recovery of the response was obtained by washing the preparation for 60 min. in the CARB- and Na-free solution. Competitive antagonists (Ba^{++} and Rb^+) of resting ^{42}K-exchange did not block the CARB stimulated ^{42}K-efflux. At equivalent doses (0.05mM) 9-aminoacridine, butacaine and lobeline completely but reversibly blocked the CARB induced response. SKF 525-A (0.05mM) completely and irreversibly (2-hr. wash) blocked the CARB stimulated ^{42}K-efflux. These findings indicate that the increase and decrease of ^{42}K-efflux is a reliable measure of cholinergic receptor activation and inactivation in the absence of depolarization. It is possible that agents which cause receptor desensitization may do so by altering ionic mechanisms (Magazanik and Vyskočil, J. Physiol. 210:507-518, 1970). (Supported by Univ. Conn. Res. Found. Grant).

TH-POS-C3 BICUCULLINE, COMPETITIVE ANTAGONIST OF THE POSTSYNAPTIC γ-AMINOBUTYRIC ACID RECEPTOR. E.J. Peck, Jr., J.M. Schaeffer* and J.H. Clark*
Cell Biology, Baylor College of Medicine, Houston, Texas 77025.

Previous studies from our laboratory have demonstrated a Na^+-independent, chlorpromazine-insensitive binding site for γ-aminobutyric acid (GABA) in synaptosomal (BBRC, 52:394, 1973) and synaptic plasma membrane (Trans. Am. Soc. Neurochem. 5:114, 1974) fractions of rat cerebellar cortex. In the present investigation this binding site, which we consider the postsynaptic GABA receptor, has been solubilized from synaptic plasma membranes and employed to study various pharmacologic agents which affect central GABA systems. L-diaminobutyric acid (500 μM), chlorpromazine (200 μM), and Na^+-free conditions, all of which inhibit tissue and synaptosomal transport of GABA, have no effect on the receptor·^{3}H-GABA interaction. ^{3}H-GABA binds with a K_d of 12 μM and a B_{max} of 0.28 pmol/μg protein. Freshly prepared solutions of bicuculline competitively inhibit the binding of ^{3}H-GABA with a K_i of 45 μM. However, the solutions stored at neutral pH for 24 hours are without effect on GABA binding. Bicuculline is unstable at neutral pH, being converted to bicucine by opening of a lactone ring. The conversion, followed at 293 nm, is a first-order process with a half-life of 2.5 hours (pH 7.3, 22°C). We conclude that failure to demonstrate inhibitory effects of bicuculline in electrophysiologic or chemical studies may result from the conversion of pharmacologically active bicuculline to inactive bicucine. Our data strongly support the contention that bicuculline is a competitive antagonist of the postsynaptic GABA receptor. (Supported by HD08389-01 and the Research Foundation).

TH-POS-C4 A COMPARISON OF REDUCED α-PARAMYOSIN WITH β-PARAMYOSIN USING TRANSIENT ELECTRIC BIREFRINGENCE. D. L. DeLaney* and S. Krause, Department of Chemistry, Rensselaer Polytechnic Institute, Troy, New York 12181.

Transient electric birefringence techniques have been used to show that the α-paramyosin molecule, both oxidized and reduced, is about 6% longer than β-paramyosin. The samples were in aqueous solution at pH 3.2 at 1-2 mM ionic strength. Birefringence relaxation data were extrapolated to infinite dilution of protein, and the lengths of the molecules were calculated assuming a diameter of 20 Å for each. A length of 1200 Å was then calculated for β-paramyosin, and 1275 Å for both oxidized and reduced α-paramyosin. The β-paramyosin was prepared from the white portion of the adductor muscle of the chowder clam Mercenaria mercenaria by an ethanol extraction procedure (Johnson et al., 1959, Science, 130, 160). Reduced α-paramyosin was prepared by a similar extraction (Stafford, Ph.D. Thesis, U. of Conn., 1973) in the presence of 0.01 M EDTA and 5 mM dithiothreitol. Oxidized α-paramyosin was prepared from the reduced protein by treatment with $CuCl_2$ and oxygen. Transient electric birefringence techniques have also been used to compare the aggregation behavior of the samples from pH 3.2 to pH 10.

TH-POS-C5 EFFECTS OF CHANGES IN CALCIUM CONCENTRATION AND pH ON THE SODIUM AND POTASSIUM CONDUCTANCES OF MYXICOLA GIANT AXONS. C. L. Schauf, Departments of Neurological Sciences and Physiology, Rush Medical College, Chicago, Illinois, 60612.

Myxicola giant axons were studied under voltage-clamp in solutions with $[Ca^{++}]$ from 2 mM to 200 mM. The magnitudes of the observed shifts in the sodium and potassium conductance-voltage curves, $G_{Na}(V)$ and $G_K(V)$, as well as the shifts in the voltage-dependent rate constants, caused by changes in $[Ca^{++}]$ were comparable and consistent with a model in which there is no binding of divalent cations to the exterior membrane surface, but there is a net negative surface charge(σ^-). Assuming a uniform distribution gives a value for σ^- of -0.013 charges/ $Å^2$. Further support for this conclusion is provided by the observation that equimolar substitution of Mg^{++} for Ca^{++} produces no appreciable shift of $G_{Na}(V)$ or $G_K(V)$. Alteration of $[Ca^{++}]$ has no effect on the shape of the steady-state sodium inactivation relation, merely causing a translation along the voltage axis. There is also no effect of $[Ca^{++}]$ on the magnitude of the sodium inactivation delay, or on the ratio of inactivation time constants measured using two-pulse experiments versus those obtained by curve fitting the responses to step depolarizations to the same potential. A surface charge model in which divalent cations do not bind is therefore adequate for Myxicola and there is no evidence supporting an intimate involvement of Ca^{++} with gating processes. Effects of pH were examined over the range 4.0-10.5. The results differ markedly from those in other systems in that both G_{Na} and G_K are relatively insensitive to decreases in external pH as low as 4.0, but are strongly and reversibly depressed by increases in pH. The inhibition begins near 8.5 and increases with increasing pH. (Supported by the Morris M.S. Research Fund)

TH-POS-C6 THE IONIC COMPONENTS OF THE CURRENT PULSES WHICH CROSS THE GROWING TIPS OF PELVETIA EMBRYOS.
Richard Nuccitelli and Lionel Jaffe, Biology Dept., Purdue University, West Lafayette, Indiana 47907

1. Using a newly developed ultrasensitive vibrating extracellular electrode, we have found that the two-celled embryo of the fucoid alga, Pelvetia, drives large current pulses through itself. Considered as a flow of positive ions, these pulses enter the embryo's growing tip and are believed to result from transient changes in the ion permeabilities of the membrane at this tip. We have explored these changes by observing the immediate effects of varying the medium's composition. 2. Na^+ and Mg^{++} are not required for pulsing. In fact, lowering external Na^+ actually stimulates very large pulses. Since tracer studies show that Ca^{++} entry is speeded by Na^+ reduction, this finding suggests that Ca^{++} entry triggers the pulses. 3. A ten-fold reduction in external Cl^- raises the pulse amplitude by 40%. This suggests that Cl^- efflux carries most of the "inward" current, and in fact is quantitatively consistent with the inference. Further evidence for Cl^- involvement comes from studies of the effects of the membrane potential on pulsing. The pulses actually reverse direction when the membrane potential is reduced from -70 to -20mV by a ten-fold increase in external K^+; they are largely suppressed (thus indicating a reversal point) when it is cut to -35mV by a five-fold increase in K^+. This reversal potential almost certainly rules out Ca^{++} as the main current carrier; but is consistent with Cl^-, if we assume the plausible value of 120 mM for the internal Cl^- activity. Pulsing is stimulated by decreases in the external osmotic pressure as small as 5%. This suggests that one function of pulsing is to regulate the internal osmotic pressure by KCL release.

TH-POS-C7 GELLATION AND CONTRACTION OF ACANTHAMOEBA EXTRACTS. T. D. Pollard, Anatomy Department, Harvard Medical School Boston.

The experiments reported here show (1) that actin in high speed extracts of Acanthamoeba undergoes a temperature dependent polymerization, which, under appropriate conditions, results in the gellation of the extract, and (2) that when the gelled extract contracts, the cell's small (180,000 dalton), globular myosin becomes associated with the actin. Amoebas are homogenized in 0.34 M sucrose, 10 mM imidazole pH 7, 0.1-1 mM ATP, 1 mM DTT and 1 mM EGTA and then centrifuged at 140,000 g for 1 hr to obtain a supernatant of soluble proteins. Actin constitutes about 10% and myosin about 0.5% of the protein in this extract, but there are no polypeptides coelectrophoresing in SDS with the heavy chain of muscle myosin. Upon warming to 24°C, the extract gels in about 30 min during which there is an increase in A_{350} of about 0.08. If the gel is ultracentrifuged at this point, much of the actin sediments, but most of the myosin remains in the supernatant. If the gel is allowed to stand at 24°C, there is a continued, but slower, increase in A_{350} over two to three hours, and, if the gel is not firmly attached to its container, it contracts with the expression of fluid to 25% or less of its original volume. The contracted gel consists of virtually all of the cell's actin and myosin, in addition to an unidentified protein of about 50,000 daltons. These findings may indicate that the Acanthamoeba "mini-myosin" is capable of interacting with actin to generate force sufficient to contract the solidified cell extract. (Supported by USPHS Grant GM-19654)

TH-POS-C8 A MODEL OF THE MOLECULAR MECHANISM OF MEMBRANE EXCITABILITY. G. Baumann, P. Mueller*, and D.O. Rudin*, Department of Molecular Biology, Eastern Pennsylvania Psychiatric Institute, Philadelphia, Pennsylvania 19129.

A molecular mechanism of membrane excitability based on the chemical properties of gating molecules such as alamethicin is proposed. Gating molecules have an elongated shape and are as long as the thickness of the bilayer. One end of the molecule is strongly attracted to the membrane surface while the other end is charged and acts as a voltage receptor. An appropriate voltage across the membrane drives the charged end into the membrane while the other end is anchored to the surface. As a result the molecules rotate by 90° to a position perpendicular to the membrane plane. In this inserted state they aggregate and form ion channels. Quantitative calculations of the kinetic behavior of such channels match the observed gating kinetics. For example, the model explains inactivation as a direct consequence of the aggregation process without any further assumptions. (This research was supported in part by Grant BMS68-00073 from the National Science Foundation.)

TH-POS-C9 Oxytocin-like effect of cyclic AMP on membrane particles distribution in frog urinary bladder. J. CHEVALIER+, J. BOURGUET and J.S.HUGON+. Inst.de Pathol.Cell.,Hôpital de Bicêtre. Dept.de Biologie,C.E.A.Saclay,France and Dept.of Pathol.Univ.of Sherbrooke, P.Q., Canada.

In a preceeding paper (Chevalier et al,Cell Tiss.Res.,1974 152,129)we have shown that the density of the associated particles seen by the freeze-etching method,is locally modified in the apical membrane of frog urinary bladder during the antidiuretic action of oxytocin.We now report some new observations on m.a.p.clustering after cyclic AMP treatment.During the present series of experiments,the bladders were treated in two ways: In the first,the bladders were used as sacs and incubated for 20 min.either at rest or in the presence of cyclic AMP 10^{-2}M,their both faces bathed with Ringer solution; In the second,the isolated epithelium of the bladder was mounted between two lucite chambers in the presence of an osmotic gradient and the net flux of water across the epithelium was measured.In both cases,the preparation were then processed for freeze etching after fixation with glutaraldehyde 2 percent for 20 min. Both in total bladder and in isolated epithelium challenged by cyclic AMP,the apical membrane A face of the epithelial cells shows the existence of small areas with increased number of m.a.p.clusters.Such areas are not observed in resting bladders and there is no indication that the presence of a net flux of water does change the appearance of these clusters. The relationship between these areas and the intensity of the hydrosmotic response is presently investigated.

TH-POS-C10 THERMAL RESPONSES TO SMALL LENGTH CHANGES IN ACTIVE MUSCLE. S.H. Gilbert and Y. Matsumoto, Emory University, Atlanta, Georgia 30322.

Earlier work has shown that small ($\Delta\ell \leq 0.5\%\ell_o$) quick releases in active muscle are accompanied by a production and absorption of extra heat that follows the time course of the tension change (Gilbert & Matsumoto, Biophy. Soc. 1974). Larger releases ($1\% \leq \Delta\ell \leq 3\%\ell_o$) are accompanied by larger amounts of extra heat with a biphasic time course. The first phase accompanies and is directly proportional to the tension change associated with the release as would be expected of thermoelastic heat. The second phase is unreversed and accompanies tension redevelopment after the length change ends. It is roughly proportional to $\Delta\ell$, as would be expected of shortening heat (h_S) produced by the shortening of a "contractile component" as tension is redeveloped. However, further examination of the time course of the second phase of heat has shown that some tension redevelopment (equivalent to a shortening of $0.5\%\ell_o$) occurs with no concomitant production of h_S, even following large releases. Thus tension recovery following a quick release occurs by two thermally distinguishable processes, only one of which produces extra heat. Small quick stretches were also found to be accompanied by a biphasic thermal response even for $\Delta\ell \leq 0.5\%\ell_o$. The first phase is an absorption of heat as tension rises and seems to be of thermoelastic origin. The second phase is an unreversed production of extra heat as tension falls. The extra heat remaining after stretch is approximately equal to the work applied during stretch but is not produced simultaneously with it. The time course of the second phase follows that predicted if a time course of "lengthening heat" during tension decay is calculated, assuming Hill's coefficient a to apply for $P > P_o$. Thus tension recovery following stretch seems to be accomplished by only one thermally characterizable process, which produces extra heat.

TH-POS-C11 LITHION ION INTERACTION WITH THE SODIUM/POTASSIUM PUMP IN FROG SARTORIUS MUSCLE. L. A. Beaugé, Department of Biophysics, University of Maryland School of Medicine, Baltimore, Maryland 21201.

The effects of $[Li]_o$ on Na and K efflux and on K influx were studied in high Na sartorius muscles. With $[Ba]_o = 0$, a change from K-free Mg to K-free Li gave an increase in both Na and K efflux; addition of ouabain inhibited Na efflux while increasing K efflux. Incubation in 2 mM Ba greatly reduced K permeability; subsequent addition of Li gave a ouabain-sensitive Na efflux 57% of that in the absence of Ba while K efflux increased only slightly and was unaffected by ouabain. Activation curves for Na efflux as a function of stimulating cation concentration in Na-free Mg-Ba Ringer were more or less hyperbolic for both K and Li. While half-maximal activation was attained at higher [Li] than [K], maximal efflux in Li was smaller than that in K. The extra Na efflux produced by K increased when Li was added; this was not a simple additive effect and was independent of [Li]. At some concentrations Li increased the ouabain-sensitive K influx, but at others reduced it. Incubation in 50 μgr/ml Nystatin gave reversible changes in membrane permeability to monovalent cations. When $[K]_i$ was reduced to ca. 1-2 μmole/gr (with Li as substituent), both $[K]_o$ and $[Li]_o$ promoted a ouabain-sensitive extra efflux of Na. Ouabain-insensitive Na efflux in (K+Na)--free solutions was not affected by removal of Ca from media in either Mg or Li solutions, both with and without Ba; values for this residual efflux were higher in Mg than in Li. The results fully support the notion that lithium ions have a potassium-like action on sodium pump in muscles. They also suggest that some other kind of interaction may exist between lithium and the sodium/potassium pump.

TH-POS-C12 THE TEMPERATURE DEPENDENCE OF CHLORIDE FLUXES IN THE SQUID GIANT AXON. V. Scruggs and D. Landowne, Department of Physiology and Biophysics, University of Miami, Miami, Florida 33152.

The influx and efflux of radioactive chloride was measured in intact squid giant axons. In the resting axon the rate of efflux was 2.8×10^{-4} min^{-1} at room temperature. When the temperature was decreased the efflux decreased with a Q_{10} of 1.3. There was no detectable extra efflux associated with nerve impulses. The resting influx at room temperature was 14 p-moles/cm^2-sec and this decreased as the temperature was lowered. The Q_{10} for the resting influx was found to be 2.4. There was an extra influx of chloride associated with nerve impulses of 0.08 p-moles/cm^2-imp. at room temperature and this increased as the temperature was lowered with a Q_{10} of 1/1.3. The ratio of the resting fluxes (influx/efflux) at low temperatures approaches what would be expected for independent, passive movement of the ion whereas at room temperature the ratio is clearly too large.

The high temperature dependence of the resting influx and the flux ratio calculations support the idea that there is an inwardly directed active transport mechanism for chloride ions in the squid axon membrane. The low temperature dependence of the extra chloride influx associated with nerve impulses is consistent with the low temperature dependence of the extra fluxes of sodium and potassium.

Supported by the National Science Foundation Grant GB-36859.

TH-POS-C13 A POSSIBLE NEW PROCESS THAT ACTS TO INCREASE TRANSMITTER RELEASE AT THE FROG NEUROMUSCULAR JUNCTION. J.E. Zengel* and K.L. Magleby, Dept.of Physiology and Biophysics, Univ. of Miami School of Med., Miami, Fla.33152

This study is directed at characterizing a third process, in addition to facilitation, F(t), and post-tetanic potentiation, P(t), which acts to increase transmitter release during and following repetitive stimulation. End-plate potentials (e.p.p.s) were recorded either intra- or extracellularly from the low Ca high Mg blocked frog neuromuscular junction. The nerve was first stimulated once every 5 sec to establish a control response, then stimulated repetitively for 300-600 impulses at 10-20/sec. Following the conditioning stimulation the decay of the resulting increase in e.p.p. amplitudes was followed with single testing impulses applied every 2 or 5 sec. When plotted against time this decay of increased e.p.p. amplitudes could be described by 2 exponential components: a faster component which we call I(t) (for intermediate process) and a slower component which represents P(t). It is not known how I(t) and P(t) interact, but assuming a multiplicative relationship the magnitude of I(t) ranged from 0.19 to 5.31 with a mean of 1.28. The magnitude of I(t) was not directly related to the magnitude of P(t) but could be greater or less depending on the stimulation parameters and preparation. I(t) was found to account for up to 40% of the increase in transmitter release during the conditioning trains. The time constant of decay of I(t) was intermediate in duration between F(t) and P(t), ranging from 2.4 to 11.5 sec with a mean of 4.6 sec. The effect of I(t) on F(t) (determined with double testing pulses) could not always be described by assuming either a multiplicative or additive relationship between I(t) and F(t), although the data were usually more closely described by assuming a multiplicative relationship, suggesting some independence of I(t) from F(t). Supported by USPHS grant NS10277.

TH-POS-C14 FILAMENT FORMATION OF SMOOTH MUSCLE MYOSIN. X. Joseph*, L. F. Lemanski, and M. R. Iyengar*, Departments of Animal Biology and Biology, University of Pennsylvania, Philadelphia, Pennsylvania 19174.

Smooth muscle myosin was prepared from bovine uteri by repeated washings with glass distilled water followed by extraction with 0.6 M KI containing 20 mM histidine. After three centrifugation and precipitation cycles, the final precipitate was dissolved in 0.6 M KCl cysteine buffer and centrifuged at 150,000 g. The upper 2/3 of the supernatant containing myosin was collected and frozen at -76° C. Sodium dodecyl sulfate (SDS) polyacrylamide gel electrophoresis of this sample showed a prominent band at 210,000 daltons indicating the presence of myosin. The preparation was virtually actin-free. Analytical ultracentrifugation experiments confirmed the presence of myosin. Electron microscopic negative staining studies of synthetic filament formation using these preparations suggest that at low ionic strength (0.1 M KCl) long thick filaments with diameters ranging from 180 Å-220 Å and some short filaments in aggregates are formed. When 5 mM magnesium and pyrophosphate (pH 7.2) are present extensive networks of long thick filaments are seen. In high ionic strength solution (0.6 M KCl), with or without magnesium and pyrophosphate, long thick filaments are not obvious; however, the addition of magnesium and pyrophosphate causes the formation of a few short segments of filaments in a loosely arranged network. It is concluded from these preliminary experiments that low salt concentration in the presence of magnesium and pyrophosphate favors the formation of long thick filaments of vertebrate smooth muscle myosin. (Supported by NIH Grant HL 15835-02 to the Pennsylvania Muscle Institute).

TH-POS-C15 EVALUATION OF ELECTRIC FIELD EFFECTS IN INTERCALATED DISK CLEFT BETWEEN MYOCARDIAL CELLS. N. Sperelakis and J.E. Mann, Jr.,* Depts. of Physiology & Applied Mathematics, University of Virginia, Charlottesville.

Two contiguous myocardial cells with a narrow junctional cleft between them (intercalated disk) and bathed in a large volume conductor were modeled by an electrical analog circuit. A circuit analysis and computer simulation was also done. Each cell was divided into four regions, each represented by lumped Hodgkin-Huxley units: (1) junctional membrane (JM) at left end of cell, (2) surface membrane (SM) at left half of cell, (3) SM at right half, and (4) JM at right end. The JMs were given the same resistivity as the SM. The radial resistance of the cleft was varied to represent different cleft widths. Firing an action potential in one JM bordering the cleft (Cell 1), by lowering its Na^+ resistance, caused the potential in the cleft to swing negative with respect to ground (fluid bath). Although the inner surface of the JM of Cell 2 remained at nearly constant potential with respect to ground, it was depolarized by the same degree as the negativity at its outer surface. The depolarization for a 200 Å cleft was beyond the hypothetical threshold potential. The electric field effect was larger the narrower the cleft. The excited JM activated the remainder of Cell 2. Thus, virtually no local-circuit current flowed through Cell 2, and it fired without low-resistance connections between the cells. However, because simultaneous firing of the right half SM of Cell 1 (unit 3) causes complete cancellation of the cleft potential, for the present model to give a workable basis for the transfer of excitation from cell to cell, unit 4 must fire a fraction of a millisecond before unit 3. (Unit 2 causes partial cancellation.) This is possible if the JM has a slightly lower threshold or K^+ accumulates in the cleft; there is also a slightly larger IR drop across unit 4 than unit 3.

TH-POS-C16 EFFECTS OF BRAIN EXCITABILITY ON THE LEVEL OF TAURINE IN RAT BRAIN. M. H. THURSBY, Dept. Physiology, State Univ. of New York at Buffalo, Buffalo, N. Y. 14214, and A. H. Nevis, Dept. Electrical Engineering, Univ. of Florida, Gainesville, Florida 32603.

The effects of taurine on the excitability of neurons in the periphery as well as the central nervous system have been studied extensively. We studied the effects of changes in excitability level as determined by quantitative abnormal EEG analysis on the endogenous taurine level in rat brain. White male Sprague-Dawley rats of uniform weight were stressed osmotically to produce abnormal EEG and behavioral patterns and were sacrificed by immersion in liquid nitrogen at various stages of seizure activity. The brains were removed and analyzed for free taurine. A low correlation (0.07) was shown between the short term abnormal activity (i.e., single epileptiform seizures) and the endogenous taurine concentration. However, the level of long term subthreshold abnormal activity as manifested in the EEG shows a high correlation (-0.7) with the taurine level. Our data suggest, first, that a long term increase in excitability of the brain due to surgical insult may have decreased the "endogenous" taurine level. Second, due to biochemical variability of brain taurine levels, a similar surgical procedure may have varying effects on the brain excitability. Although the taurine levels remain relatively constant during seizures, this does not preclude metabolically related compounds (e.g., isethionic acid, ISA) from changing concentration and thus affecting the ionic distribution across the membrane and, hence, membrane excitability.

TH-POS-C17 CHEMICAL REACTIVITY OF AMINO ACIDS WITH LASER GENERATED SINGLET MOLECULAR OXYGEN. Dale E. Brabham*, I.B.C. Matheson* and John Lee (Intr. by John M. Brewer), Department of Biochemistry, Univ. of Georgia, Athens, Georgia 30602.

The total physical and chemical quenching of laser generated singlet molecular oxygen by amino acids has been previously determined in D_2O by studying the kinetics of the reaction of bilirubin and singlet oxygen in the presence of amino acids.[1] Current work attempts to distinguish between physical and chemical terms in the overall quenching process by measuring the chemical rate of loss of amino acid directly. The amino acid in D_2O at millimolar concentration under 130 atm oxygen, was irradiated 1 to 5 min with a Nd-YAG laser at 5 to 6 watts CW. The 1.06 μm output of the laser, excites molecular oxygen into its $^1\Delta_g$ state. The amino acid was assayed immediately after the singlet oxygen treatment with a ninhydrin test according to the method of Lee and Takahashi.[2] The relative reactivities of different amino acids measured by this method are compared to the relative quenching rates previously determined. The impact of these results on interpretation of dye sensitized photooxidation of proteins and amino acids is presented. Supported by grants of NIH (HD 07714-02), NSF (GP-38218X1) and Public Health Service Research Grant No. CA 00503 (to D.E.B.) from the National Cancer Institute.

1. I.B.C. Matheson, R.D. Etheridge, Nancy R. Kratowich and John Lee, Photochem. Photobiol., in press (1975).
2. Ya Pin Lee and Tunekazu Takahashi, Anal. Biochem. 14, 74 (1966).

TH-POS-C18 FURTHER EVIDENCE THAT SH_1-BLOCKED HMM (NEM-HMM) EXISTS IN A REFRACTORY STATE DURING INTERACTION WITH ACTIN AND ATP. Sally Mulhern, Evan Eisenberg and W. Wayne Kielley, NIH, Bethesda, Md. 20014

In previous studies we demonstrated that as with unmodified HMM very little NEM-HMM is bound to actin during ATP hydrolysis under conditions of maximum actin activation. From this it was suggested that during the cycle of interaction with actin and ATP, NEM-HMM underwent a rate limiting conversion from the refractory state which is unable to bind to actin to the non-refractory state which can bind to actin. This model predicts that as with unmodified HMM the ATP turnover rate per mole of actin at high [NEM-HMM] would be much higher than the ATP turnover rate per mole of NEM-HMM at high [actin]. Double-reciprocal plots of the ATPase rate at high [NEM-HMM] or high [actin] demonstrated that the ATP turnover rate per mole of actin was about 10-fold higher than the ATP turnover rate per mole of NEM-HMM. Thus it appears that during the cycle only a small part of the NEM-HMM is bound to actin at high [actin]. This conclusion depends on there being only one species of modified HMM present, i.e. it must be demonstrated that NEM-HMM unbound to actin during ATP hydrolysis has the same ATPase activity as the original NEM-HMM. This was demonstrated by showing that the unbound HMM had the same 3-fold maximum actin activation just as the original NEM-HMM. We isolated the HMM which remained unbound to actin by using an analytical ultracentrifuge equipped with a separation cell which separated the HMM which remained unbound to actin during ATP hydrolysis. Therefore, the NEM-HMM does not appear to consist of two separate species,only one of which binds to actin and shows actin activation. Rather it is a single species which undergoes a rate-limiting transition from the refractory to the non-refractory state during interaction with actin and ATP.

TH-POS-C19 VARIATIONS IN INTERNAL RESISTIVITY WITH SARCOMERE LENGTH IN FROG SEMITENDINOSUS FIBERS. A. Dulhunty* and C. Franzini-Armstrong* (Intr. by H. Eberle). Dept. of Physiology, University of Rochester, Rochester N.Y. 14642.

The internal resistivity of muscle fibers, as measured in standard cable analysis (R_i) depends on two factors a) the volume of conducting electrolyte per unit length of fiber, and b) the geometry of internal structures, i.e., the sarcoplasmic reticulum and fibrils. Both factors might be expected to vary as the fiber is stretched. We have measured R_i as a function of sarcomere length (S) in single fibers isolated from semitendinosus muscles of Rana pipiens. The sarcomere length was measured during the experiment from a laser beam diffraction pattern. Electrical parameters were determined by standard cable analysis. The fiber cross section was measured optically. To avoid damage and length changes during transfer to the optical system, the fibers were fixed in 0.1 % glutaraldehyde in Ringer's following electrical measurements. This concentration of glutaraldehyde produces no shrinkage or shape changes. R_i from at least 8 fibers was measured at each sarcomere length (S= 2.2, 2.5, 2.9, 3.1, 3.5, 3.8 and 4.2 μm), T=26°C. We find that R_i increases with sarcomere length from a value of 122±3.03 cm (mean± 1 SEM) at S= 2.2 μm to 238±20 cm at S= 3.8μm. The increase in R_i with S is approximately linear between 2.2 and 3.8 μm. We calculate that the increase in resistivity cannot be simply explained by changes in thin and thick filament packing, since the increased packing density during stretch is counterbalanced by a decrease in the area of overlap. A change in Ri may be produced by rearrengement of the sarcoplasmic reticulum and/or distortion of the Z line substructure.

Supported by grants from the Muscular Dystrophy Association of America and from NIH, IPO INS 10981-02.

TH-POS-C20 VOLTAGE NOISE AND IMPEDANCE FROM HEART CELL AGGREGATES L. J. DeFelice and R. L. DeHaan, Department of Anatomy, Emory University, Atlanta, Georgia, 30322

Voltage noise has been recorded from spheroidal aggregates of embryonic chick heart cells maintained in tissue culture. Spontaneous action potentials were suppressed, but not wholly eliminated, with tetrodotoxin. Steady-state noise, at resting potentials from -60 to -80 mV, was monitored simultaneously from 2MKCl filled glass microelectrodes in two different cells in an aggregate. Aggregate impedance was measured by injecting dc and ac current through one electrode.

The degree of electrical coupling between cells in an aggregate could be determined independently by cross-correlation of the spontaneous voltage noise records, and from the impedance measurements. An index of coupling based on the noise measurements may be defined as the ratio $C12/(C11C22)^{1/2}$ where C12 is the cross-correlation of the voltage noise from the two electrodes, and C11 and C22 represent the autocorrelation of noise from each cell. This method provides a novel estimate of cell coupling without injection of current. It demonstrates that heart cells are normally well coupled, but that the degree of coupling is frequency dependent and may change with time.

Aggregate impedance exhibits a resonance near 1 Hertz, depending on mean membrane potential and aggregate size. From the voltage noise and impedance data it is possible to derive kinetic properties of the excitable heart cell membrane.

TH-POS-C21 SYSTEM ANALYSIS AND ELECTRONIC SIMULATION OF THE LIGHT GROWTH RESPONSE OF PHYCOMYCES. E. D. Lipson* (Intr. by Max Delbrück), Division of Biology, California Institute of Technology, Pasadena, California 91125.

The white noise method (Marmarelis and Naka, J. Neurophysiol. 36: 605-648, 1973) has been used to identify Wiener kernels of the Phycomyces light growth response system. The response is reasonably linear with the logarithm of light intensity over the range of a few decades. Analysis of the first-order kernel by linear system theory has permitted the design of a simple electronic circuit which accurately simulates the characteristics of the system in the normal intensity range. This circuit consists of a high-pass (adaptive) filter followed by an underdamped fourth-order low-pass filter. By replacing the first filter with a nonlinear high-pass filter, the circuit can be made to represent additionally the large range dark and light adaptation of the organism. A combined analysis of kernels for normal and high intensity levels is interpretable in terms of a first-order kinetics model for pigment bleaching and regeneration. As a consequence, the addition of a variable lead-lag filter to the input of the circuit generalizes its validity to include the high intensity range. The analysis and accompanying electronics provide insight into the system dynamics and help in designing further experimental tests of the models.

TH-POS-C22 INTERACTION OF SPECTRIN WITH ACTIN AND HEAVY MEROMYOSIN. F.H. Kirkpatrick and P.L. La Celle, Department of Radiation Biology and Biophysics, University of Rochester School of Medicine and Dentistry, Rochester, New York 14642.

Sheetz, Painter, and Singer (Ann. Rev. Biochem. 43:814, 1974) suggest that "Band 5" from erythrocytes is actin. This claim is supported by Haley and Hoffman's (P.N.A.S. 71:3367, 1974) results with photoaffinity ATP labelling and our results with high-resolution SDS-polyacrylamide gel electrophoresis. Tilney (J. Cell Biol. 63:249a, 1974) found by viscometry that skeletal muscle actin and spectrin interact.

We find that skeletal muscle actin alters the cation optima and activity of the ATPase activities of spectrin, and the results depend on whether the actin is polymerized (F) or depolymerized (G). F-actin partially inhibits the ATPase of spectrin at high calcium levels, lowers the cation optimum for Mg-ATPase of spectrin, and has effects on the low-calcium (1 mM) ATPase of spectrin that depend on the magnesium concentration. G-actin inhibits both spectrin calcium-ATPases, but does not affect the Mg-ATPase. Electron microscopy of negatively-stained samples shows that spectrin appears to bind to F-actin, and that F-actin may stimulate the polymerization of spectrin into its characteristic fibrils. G-actin may partially inhibit spectrin polymerization.

Heavy meromyosin (HMM) appears by electron microscopy to interact with spectrin, but HMM ATPase is not affected by spectrin, and HMM ATPase obscures effects of HMM on spectrin ATPase. (Supported by NIH grant HL16421-04 and by U.S. AEC contract with the University of Rochester Atomic Energy Project and has been assigned Publication Number UR-3490-647.)

TH-POS-C23 UNUSUALLY LOW POTASSIUM PERMEABILITIES IN WINTER FROGS. Mary Jacobs McCrea, Departments of Ophthalmology and Physiology, George Washington University Medical School, Washington, D.C., 20037.

Unusually low relative potassium conductances have been observed in apparently healthy frogs during the winter season. The rapid ion shift method was used to determine the relative conductances to potassium, sodium, and chloride of the frog sartorius. Membrane potentials averaged 68.14 $\pm$ 7.03 mv in 14 fibers from 11 frogs. A fourfold or twofold (adjusted) increase in extracellular potassium resulted in a shift of membrane potential averaging 0.79$\pm$0.66 mv giving a calculated transport number of 0.023 $\pm$ 0.019. A switch to half chloride solution produced a change averaging 9.88$\pm$1.83 mv with a calculated transport number of 0.56$\pm$0.105. Thus these winter frogs apparently shut down potassium permeability and the membrane potential is maintained by chloride ions. In one muscle shifts were measured at intervals of 0.2 pH units from pH 7 to 10.4. Two others were measured from 7 to 6.0 and 5.6. Potassium shifts were close to 0 throughout the range indicating that there is no loosening of the membrane at alkaline pH. Chloride shifts increased with increasing pH from 6 to 9. The resistance decreased with pH below 8.0 The sum of the transport numbers was 1 only in the extreme alkaline range.

TH-POS-C24 AN EXTENSION OF CABLE THEORY TO A MULTICELLULAR TISSUE. Eric Jakobsson and Lloyd Barr, Department of Physiology and Biophysics, University of Illinois, Urbana, Illinois 61801.

The one-dimensional theory of an infinite cable which is used to describe electronic current spread along an axon has been extended to a particular three-dimensional situation; namely a multicellular tissue anisotropic in one dimension. It is assumed that the intra and extracellular resistivities of the tissue are different perpendicular and parallel to the long axis of aligned cells (such as muscle cells). A vector formalism is used to derive equations describing the voltage distribution in the tissue as a function of intra- and extra-cellular and transmembrane resistivity. One of the major results derived is that for the case in which current is injected into a cell at a point and withdrawn from extracellular space at the same point, the transmembrane potential is given by

$$V_m = \frac{\lambda_r V_m(\lambda_r)}{\rho} e^{(\lambda_r - \rho)/\lambda_r}$$

where $\rho \equiv \sqrt{r^2 + (\lambda_r/\lambda_z)^2 z^2}$, in which r and z are distances from the point of current injection across and along the long axis of the aligned cells, respectively; and λ_z and λ_r are functions of transmembrane and tissue resisitivity along and across the axis of the aligned cells, respectively. λ_z and λ_r are close analogs to the length constant in one-dimensional cable theory. V_m (λ_r) is the transmembrane potential measured at $\rho = \lambda_r$.

This work was supported by Grant No. HL14125 from the Heart and Lung Institute of the National Institutes of Health.

TH-POS-C25 COOPERATIVE TRANSITIONS IN IONIC PERMEABILITY IN CRAYFISH AXON MEMBRANES RESULTING FROM CHANGES IN EXTERNAL CALCIUM AND POTASSIUM.
A. Strickholm, and H.R.Clark*, Anatomy-Physiology Department, Indiana University, Bloomington, Indiana 47401

Membrane conductance and the dependence of membrane potential on specific external ions (transference number) was measured in crayfish (Procambarus clarkii) giant medial axons. In neutral to alkaline pH, where potassium membrane permeability dominates, a graph of the logarithm of conductance (G_o) against the logarithm of external potassium (K_o) shows a linear relation. However, near an external potassium concentration of 14 mM (V_m = -60 mV), a marked change occurs in membrane conductance over a few mM of K_o which shifts the relationship between log(G) and log(K_o). In alkaline pH, the transition typically involves only a step change in conductance with no change in the slope of log(G) vs log(K_o). In addition, the relative potassium to chloride conductance is reduced. In acid pH, where chloride conductance is contributory, the slope relationship may change. Similarly, conductance transitions are also found upon altering external calcium ions (Ca_o). A plot of log(G) vs log(Ca_o) ordinarily plots linearly. However, a marked change in the slope of log(G) vs log(Ca_o) appears around a calcium concentration of 13 mM in normal saline. These results are interpreted as indicating that a surface membrane cooperative conformational change occurs in the ionic permeability regulating components at critical potassium and calcium concentrations.

TH-POS-C26 A LARGE CHANGE IN AXON ABSORPTION DURING THE ACTION POTENTIAL
W.N. Ross*, B.M. Salzberg, L.B. Cohen, H.V. Davila*, A.S. Waggoner and C.H. Wang*. Dept. of Physiology, Yale University, New Haven, Conn. 06510 and Dept. of Chemistry, Amherst College, Amherst, Mass.

Absorption changes of several dyes, applied externally, were evaluated for their sensitivity as indicators of membrane potential during neuronal activity. Giant axons from the squid, Loligo Pealii, were cleaned and placed horizontally in a chamber on a microscope stage. The axons were dyed for 20 minutes in a sea water solution of the dye and then washed in sea water bubbled with argon. Quasi-monochromatic light passing through a 150 um length of axon was focused on a photodiode and the change in absorption recorded during the action potential. With two dyes, "merocyanine 540" (Eastman Organic Chemicals) and its 1,3-dihexylthiobarbituric acid derivative, the increase in absorbance during a single action potential could be detected with a signal-to-noise ratio of about 20:1. The signal was much larger than the signals found thus far in measurements of birefringence, light scattering and fluorescence on the same apparatus. For this dye the absorption increased during the action potential for incident light of 550-600 nm and decreased for light of 450-550 nm. Fluorescence signals measured with the same dyes showed increases at all excitation wavelengths. These observations are consistent with the dye existing in the membrane in both monomer and dimer forms, with the equilibrium shifting towards the monomer during depolarization. We hope that these larger signals will facilitate the development of an optical system for simultaneous recording of activity in many neurons.

Supported in part by Public Health Service grants NS 08437 and NS 10489 and NIH fellowship 1 F22 NS 00927.

TH-POS-C27 THE EFFECTS OF γ-RADIATION ON SOLUTIONS OF ACETYLCHOLINESTERASE. Nayar, G.N.A* and Srinivasan, S. Department of Biophysics, Institute of Medical Sciences, Banaras Hindu University, Varanasi, 221005, India.

Dilute solutions of bovine erythrocyte acetylcholinesterase (EC 3.1.1.7) were irradiated with Co-60 radiation under air at a temperature of around 5°C. The doses employed were approximately 30, 60, 90 and 120 krads. Biological activities were estimated before and after irradiation by the DTNB method. The activity decrease was in a conventional exponential fashion. The D-37 dose turned out to be 90 krads. UV absorption measurements in the wavelength region 230 to 330 nm resulted in the decrease of the ratio of OD(280) to OD(250). From an analysis of the difference spectra it can be shown that probably tyrosine groups are exposed as a result of irradiation. Sephadex G-200 gel filtration studies showed that there was no difference in the molecular weight of the enzyme after irradiation with 30 krads, whereas after an irradiation with 120 krads, the enzyme dissociated into two smaller particles of molecular weight of around 73,000 and 7,500. These studies show that there is probably a progressive conformational change of the enzyme at all dose levels studied. However, the change in the molecular weight is apparent only after irradiation with doses of 120 krads. It can be shown that H atom is mainly responsible for the disaggregation of the enzyme as a result of irradiation, while it is possible that OH^- and e^- are possibly involved in the activity and spectral changes.

TH-POS-D1 CARCINOGEN FREE RADICALS: OBSERVATIONS ON THE HORSE RADISH PEROXIDASE HYDROPEROXIDE GENERATION OF THE NITROXYL RADICAL OF N-HYDROXY-ACETYAMINOFLUORENE. Robert A. Floyd, Okla. Med. Res. Fndn., Okla. City, Okla. 73104.

The concentration of the nitroxyl radical generated by excess hydroperoxide, N-hydroxy-acetyamino-flourene (N-OH-AAF) and horse radish peroxidase (HRP) was determined by electron spin resonance techniques. The time course of the steady state level of nitroxyl radical was influenced dramatically by the electron donors ascorbate, reduced glutathione and tetramethylphenylenediamine but not by hydroquinone and ferrocyanide. Optical studies on the same system using much lower levels of hydroperoxide demonstrated that after each pulse of hydroperoxide there was a concomitant absorbance increase at 380nm. The absorbance increase is interpreted as due to one of the products of the reactions, 2-nitrosofluorene. The product remained in the trichloroacetic acid precipitated enzyme, but was extractable with chloroform (364nm absorption maximum). Using low level hydroperoxide pulses ascorbate prevents product formation. Kinetic experiments using HRP compound 1 and 2 are underway. (This research was initiated at Washington University, St. Louis, Mo., funded by grant 5-R01-CA03983-15 from the NIH.

TH-POS-D2 THE FLUORESCENT DRUG OLIVOMYCIN AS A PROBE FOR DNA IN THE CELL. V. W. Burns, Department of Physiological Sciences, University of California, Davis, California 95616.

The drug olivomycin is fluorescent and complexes to DNA but not to RNA. When olivomycin complexes to DNA the fluorescence intensity is enhanced, the excitation wave-length maximum shifts 15 nm, the fluorescence polarization doubles approximately, and the emission spectrum broadens and shows two maxima. The polarization of the complex increases still further if the rotation of olivomycin is impeded. Olivomycin at low concentrations is taken up efficiently by HeLa carcinoma cells, but not by BHK cells. In live HeLa cells the fluorescence is limited to the nucleus and the characteristics indicate that the drug is entirely complexed to DNA and that rotation is slowed mainly by the connection to DNA and very little by other environmental factors.

TH-POS-D3 EFFECT OF D_2O ON MELTING OF NUCLEIC ACIDS. Richard D. Blake
Department of Biochemistry, University of Maine, Orono, Maine.

The equilibrium solvent isotope effect on the thermally induced helix-coil transition of various nucleic acids has been reexamined. Sensitive temperature derivative profiles of the loss of UV hypochromicity near 260nm were obtained with a minicomputer programmed with simple algorithms for signal averaging, local curve smoothing etc., as previously described [Blake, (1973) Biophys. Chem. 1, 24]. Results under many different conditions indicate that $T_m^{D2O} - T_m^{H2O} \approx 1.6^oC$, or that only slightly more thermal energy is needed for dissociation of nucleic acid helices in D_2O. Although a ΔT_m of 1.6^o is essentially in qualitative agreement with limited earlier results suggesting no difference, this difference clearly conflicts with the extensive results of Lewin et al. [e.g. (1967), J. Theoret. Biol. 17, 181] indicating ΔT_ms' of 10-16°C at low ionic strength. We suspect that the large differences in ΔT_m at low ionic strength reported by Lewin et al. are due to trace metallic ion contamination of commercial D_2O used without further distillation. Within $\pm$ 0.5°C the observed ΔT_m is independent of 1) the number of intrabase hydrogen (deuterium) bonds, that is, the G-C content, 2) the ionic strength, and 3) temperature. We infer from our results that the free energy of transfer from H_2O to D_2O is about -35cal/mol b.p., but not necessarily entropic in origin. Various enthalpic-entropic processes undoubtedly compensate to yield the observed result; for example, the difference in dielectric between D_2O and H_2O and the difference in residual secondary structure of dissociated polynucleotides. Detailed statistical thermodynamic analyses are under way on melting profiles of poly (A)•poly(U) obtained in D_2O and H_2O in an attempt to pin down some of these questions.

TH-POS-D4 STUDIES ON THE INTERACTION BETWEEN THE fd GENE 5 PROTEIN AND NUCLEIC ACIDS. A. K. Dunker[1], E. A. Anderson*, Department of Molecular Biophysics, Yale University, New Haven, Connecticut 06520.

DNA-cellulose chromatography has been used to investigate the interaction between single-stranded nucleic acids and the gene 5 protein (5P) of the fd filamentous bacterial virus. (5P promotes virus DNA synthesis in vivo by complexing with viral, but not complementary, DNA; during virus maturation, 5P is displaced by coat protein.) Over the pH range 10.0 to 10.5, the 5P•DNA complex becomes efficiently destabilized. Parallel titrations (total and spectrophotometric) demonstrate that about 0.5 tirosines and 4 lysines are titrated from 10 to 10.5. In the acid region, from pH 5 to 4, the 5P•DNA complex becomes resistant to 1 M NaCl. 5P binding to cellulose-bound DNA in competition with free DNA suggest that free tetranucleotides do not compete with bound DNA whereas free fd DNA competes very effectively. Since the stoichiometry of the 5P•DNA complex is one molecule of 5P per 4 nucleotides, the competition experiment supports the importance of cooperative interactions. A Poisson analysis of a 5P•DNA filter binding assay in which the ratio of 5P/DNA is varied lends additional support to the importance of cooperative interactions. Competition experiments using free R_{17} RNA suggest measurable but weak 5P binding to RNA. Finally, a modified competition experiment yields 1.3 x 10^6 M^{-1} for the 5P•DNA binding constant.

Support: NSF grant GB20819 and USPHS grant AI06524 to Dr. D. A. Marvin.
[1]Present address: Sloan-Kettering Institute for Cancer Research, New York, N. Y. 10021

TH-POS-D5 MODEL OF SINGLE-STRANDED INTEGRATION OF ONCOGENIC VIRAL GENOMES. John H. Frenster, Department of Medicine, Stanford University, Stanford, California 94305.

Oncogenic viral genomes consist of at least two types of base sequences (1) sequences unique to neoplastic cells transformed by the virus and (2) sequences common to both neoplastic cells and normal cells (Proc. Nat. Acad. Sci. 70, 2629 (1973). The common sequences permit base-pairing between single strands of the viral genome and the genome of the susceptible host, freeing the resultant single strands of the host genome for messenger RNA during the gene de-repression associated with the neoplastic state (New Eng. J. Med. 288, 1224 (1973). The unpaired portions of the pairing strands are potential sites of strand scission following BUDR or radiation (Int. J. Rad. Biol. 24, 517 (1973), allowing release of the viral genome with reversion of the neoplastic cells toward normal phenotypic behavior (Virology 56, 152 (1973). RNA synthesis on the viral genome is restricted to unpaired strands of the viral genome as long as the virus remains integrated to the host genome (Proc. Nat. Acad. Sci. 70, 2304 (1973).

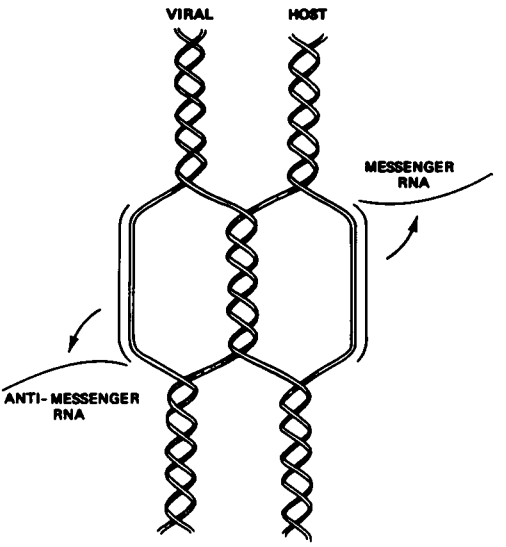

TH-POS-D6 A THERMAL DENATURATION ASSAY FOR SINGLE STRAND BREAKS IN DNA. A.T. Ansevin and D.L. Vizard, Department of Physics, M.D. Anderson Hospital & Tumor Institute of The University of Texas System Cancer Center, Houston, Texas 77025.

Damage induced by ionizing radiation in dilute solutions of chromatin or DNA includes single strand breaks, double strand breaks, and modifications to the intact helical structure of DNA evidenced by a decrease in thermal stability. Thermal denaturation profiles of the first derivative of hyperchromicity vs. the temperature reveal regular changes in profile shape as the radiation dose is increased, including skewing, decrease in the Tm, and decrease of the peak height. Both the decrease in Tm and the reciprocal of the peak height varied linearly with dose, but the latter was found to be more reproducible. The possible nature of this helix damage was investigated by comparing radiation-induced changes to those caused by double strand breaks from sonication or to single strand breakage induced by nuclease attack or by depurination and subsequent chain cleavage. Analytical sedimentation revealed that the single strand, number average molecular weight of the DNA preparations is closely related to both Tm and the reciprocal maximum of derivative thermal denaturation profiles. It is concluded that all signs of helix damage detected in the thermal denaturation assay at moderately low radiation doses result primarily from the introduction of random single strand breaks. It follows that thermal denaturation, especially employing the reciprocal maximum ordinate of a normalized denaturation profile, can be used as a convenient assay for the number of single strand breaks in free DNA or chromatin when the number average size of single strands is in the molecular weight range from about 10^4 to 2 x 10^6. Supported by USAEC contract #AT-(40-1)-2832.

TH-POS-D7 SUBUNIT STRUCTURE IN YEAST CHROMATIN. Dennis Lohr* and K. E. Van Holde, Department of Biochemistry and Biophysics, Oregon State University, Corvallis, Oregon 97331.

Staphylococcal nuclease digestion of yeast chromatin in isolated nuclei or in crude chromatin prepared from yeast nuclei produces DNA of discrete size classes. Polyacrylamide gel electrophoresis reveals that these classes are integral multiples of one basic size class or monomer, which contains about 140 base pairs. The bands are sharp; the monomer band, for example, has a width at half-height of only about 20 base pairs. Nuclei and chromatin yield identical size classes, but the rate of digestion is much greater in chromatin preparations. The time course of the digestion shows that the larger size classes are progressively degraded and the nuclease resistant monomer progressively increases in amount as digestion proceeds. Much of the yeast genome appears to be incorporated into this kind of multi-subunit structure.

The presence of subunit structure in yeast chromatin has two important consequences: (1) This kind of structural organization must be widespread in eukaryotes (2) Since yeast chromatin contains no histone f1, and probably no histone f3, the presence of these histones is not necessary for subunit organization.

This research was supported in part by a grant (GB 37307 X) from the National Science Foundation.

TH-POS-D8 LOGICAL AND PHYSICAL PROBABILITY MODELS FOR THE ORIGIN OF THE GENETIC CODE. V. Bedian*, S. Colombano*, and H. H. Pattee, Department of Biophysical Sciences and Center for Theoretical Biology, State University of New York at Buffalo, Amherst, New York 14226.

Of the two general theories for the origin of the genetic code, the structural and frozen accident theories, only the frozen accident theory can be studied usefully by simulation. To study the relevance of logical properties for the origin of a self-coding, self-replicating system we have simulated the growth of a catalytic copolymer system with randomly chosen initial sequences of copolymers and randomly chosen input and output catalytic specificities. The substrate binding strengths and the "gene" and "enzyme" initial concentrations are also chosen randomly. A probabilistic production-decay procedure is followed. Computer simulation of this model condenses to a unique translation and replication code when descriptor kinetics is sufficiently slower than constructor kinetics. The model represents a primitive self-reproducing system. Initially many self-coding subsets and codes exist, but only one survives. All enzyme concentrations, except those executing the codes decay to small values. The remaining enzymes and genes reproduce themselves under an unambiguous, complete code. This property is defined as self-coding. The consistency and completeness of self-coding acts as a logical selection pressure. By interpreting the probabilistic procedures in the model as physical fluctuations, we can argue that the logical probability of a code decreases rapidly with number of monomer types. By contrast it is chemically plausible that the probability of copolymers with reliable function and specificity initially increases with length of copolymers and number of monomer types. Such combined logical and physical models therefore provide criteria for optimum initial values of these numbers.

TH-POS-D9 ANOTHER LOOK AT NEAREST NEIGHBOR FREQUENCIES: DNA AS A TWO-SYMBOL INFORMATION TAPE. James R. White, Department of Biochemistry, School of Medicine, University of North Carolina, Chapel Hill, North Carolina 27514

DNA can be considered as a two-symbol information tape in three different ways: (1) on the "g-tape" the symbols are g (=G or C) and $\bar{g}$ (=A or T); (2) on the "p-tape" the symbols are p (=G or A) and $\bar{p}$ (=C or T); (3) on the "q-tape" the symbols are q (=G or T) and $\bar{q}$ (=A or C). The single-strand frequencies of the symbols g and $\bar{g}$, and of the doublets gg, $\bar{g}\bar{g}$, and $g\bar{g}$ (=$\bar{g}g$) are obtainable from double-strand nearest neighbor data. For instance the frequency of gg in either single-strand is the sum of the frequencies of GG, GC, CG, and CC in the double-strand. Application of information theory to these frequencies for a wide range of DNA's shows that within experimental error the occurrence of g or $\bar{g}$ is uninfluenced by its neighbor, i.e. at the doublet level the symbols g and $\bar{g}$ occur independently on the g-tape. For the p- and q- tapes, the only frequencies available are those of the self-complementary doublets $p\bar{p}$ (= $\bar{p}p$) and $q\bar{q}$ (= $\bar{q}q$). In DNA of high G + C, the occurrence of the doublets $p\bar{p}$ and $q\bar{q}$ is significantly greater than would be expected if the symbols occurred independently. For the case of low G + C no firm statement can be made about independence of the symbols on the p- and q-tapes. If one assumes that, as on the g- tape, they occur independently, then one can calculate (in favorable cases) the frequencies of the four bases on each strand of the DNA.

TH-POS-D10 C(5)-PHOTOEXCHANGE AND PYRIMIDINE ADDUCT FORMATION IN POLYDEOXYCYTIDINE. W.W. Hauswirth* and S.Y. Wang*, (Intr. by R.M. Herriott), Department of Biochemical and Biophysical Sciences, The Johns Hopkins University, Baltimore, Md. 21205

The photochemistry of the deoxycytidine excited singlet is investigated in poly dC, poly dC·dG, poly dC·rG and poly dC·rI. The kinetics of two singlet derived processes are followed. (1) Photoexchange is assayed by light induced release of a C(5)- tritium label from synthetic poly(dC-5T). From studies on the mononucleotide, photoexchange appears to require interaction between a water molecule and the excited singlet and hence its efficiency may be indicative of solvent accessibility to the C(5)-C(6) pyrimidine region in polynucleotides. (2) Formation of Cytidine(6-4')Pyrimidin-2-one (Cytidine adduct) within the poly dC chain, is assayed by its fluorescence emission and presumably does not require excited state reaction with water. Relative to poly dC, the efficiency of adduct formation in duplex polynucleotides is not greatly reduced, suggesting that no major singlet quenching mechanism is introduced upon annealing a complement to poly dC. On the other hand, at low doses C(5)-photoexchange is slow in double stranded polymers relative to poly dC-5T. At higher doses C(5)-photoexchange becomes about equally efficient to that in poly(dC-5T) alone, implying that denaturation of the duplex structure is required for solvent interaction leading to C(5)-photoexchange. Supported by NCI Fellowship 6-F22-CA02369-01 and USAEC contract AT(11-1)-3276, identified as No. COO-3276-14(76).

TH-POS-D11 PROXIMITY RELATIONSHIPS IN RNA POLYMERASE OF E. COLI. Z. Hillel, L.R. Yarbrough, F.Y.-H. Wu and C.W. Wu, Department of Biophysics, Albert Einstein College of Medicine, Bronx, N. Y. 10461.

Sigma subunit of E. coli RNA polymerase is known to stimulate specific RNA-chain initiation. Rifampicin,an inhibitor of RNA chain initiation, binds to a single site on the β subunit of RNA polymerase. We have used the energy transfer technique to deduce proximity relationships of sigma subunit and the rifampicin binding site on the enzyme. Isolated sigma subunit was covalently labeled with fluorescent donors in two ways: specific labeling of a single sulfhydryl residue with N-(iodoacetylaminoethyl) -1-naphthylamine-5-sulfonate (1,5 I-AENS) and non-specific labeling on the surface of the protein with dansyl chloride (DANS-Cl) adsorbed on celite. The labeled sigma subunits were biologically active and formed a stoichiometric complex with core polymerase. The efficiency of energy transfer was obtained from the fluorescence intensity of the sigma-labeled holoenzyme in the presence and abscence of rifampicin, which served as an energy acceptor. The transfer efficiency ($\leq$ 4%) from AENS to rifampicin gave the lower limit of the distance between the specific sulfhydryl group on sigma subunit and the rifampicin binding site to be 48 Å. It was assumed that the orientation of the donor randomized rapidly during the excited-state lifetime while that of the acceptor was fixed at some unknown angle. This assumption was supported by nanosecond emission anisotropy data. The efficiency measured for energy transfer from DANS to rifampicin was 10% in the presence of 0.2 M KCl. The distance from the surface of σ subunit to the rifampicin binding site was calculated to be 32 Å for a model having a randomly distributed and oriented array of fixed donors on the surface of a spherical σ subunit of 31 Å radius. The uncertainty in the calculated distance due to the orientation ambiguity of the acceptor was about 15%.

TH-POS-D12 RELATION OF BASE STACKING AND OPTICAL PROPERTIES OF A MODEL DINUCLEOSIDE MONOPHOSPHATE: CpC. A. Warshel and N.R. Kallenbach Dept. of Chemical Physics, Weizmann Institute, Rehovot, Israel and Dept. of Biology University of Pennsylvania, Phila., Pa. 19174.

An analysis of stacking in the model dinucleoside monophosphate CpC has been carried out in an attempt to interpret the observed changes in absorbance and CD as a function of temperature in terms of conformational changes in the molecule and the interamolecular potential governing them. The calculations were based on consistent force field empirical potential functions including the π electron system in cytosine. Contrary to previous investigations of simplified dynamical models for dinucleoside phosphates, it is concluded that hyperchromicity accompanying unstacking of CpC is incompatible with any realistic potential with a single minimum, excluding the possibility that "one-state" oscillator models for dimers can account for the thermal behavior of the optical properties. Two (or more) state models can readily explain the observed profiles on the other hand. It is suggested that dielectric screening of the solvent is important in permitting base stacking interactions to occur.
Supported by grant NSF GB 29210.

TH-POS-D13 REACTION OF DNA WITH POLYPEPTIDES. STABLE AND METASTABLE STRUCTURES. Yong A. Shin* and Gunther L. Eichhorn, Gerontology Research Center, NIH, Baltimore City Hospitals, Baltimore, Md. 21224

The formation of complexes between DNA and polypeptides can be accomplished in the following ways: (1) directly mixing (DM) the two components in the presence of excess polypeptide, and (2) prior mixing of the components at a high ionic strength which keeps them from complexing, followed by gradient dialysis (GD) to bring the ionic strength to complexing conditions. The circular dichroism (CD) of the DNA-polylysine complex produced by GD is totally different from that produced by DM. Preparations of complexes of DNA with polypeptides containing lysine in combination with one of four other amino acids, alanine, tyrosine, phenylalanine, and serine, all produce different structures by GD and DM techniques. In sharp contrast the same complex, as determined by CD characteristics, is obtained by either DM or GD from DNA and histone I. We believe that GD, through gradual formation of complex, produces a thermodynamically more stable form of the complex, and therefore assume that this stable form is also produced with the histone complex formed by DM. The DM technique, on the other hand, appears to lead to metastable forms of DNA complexes of the synthetic polypeptides studied. We postulate that such metastable forms arise from the rapid association of high concentrations of polypeptides with DNA. The structure of histone I is such, however, that rapid association with DNA produces the thermodynamically more stable form of the complex. The CD and melting characteristics of the DNA complexes of the mixed polypeptides are generally different from those of DNA-polylysine; the only similarity lies in the fact that GD and DM produce complexes of different structure.

TH-POS-D14 INTERACTION OF RIFAMPICIN WITH RNA POLYMERASE OF E. COLI. L. R. Yarbrough and C. W. Wu, Department of Biophysics, Albert Einstein College of Medicine, Bronx, N. Y. 10461.

Rifampicin, a specific inhibitor of RNA chain initiation, binds to a single site on RNA polymerase. We have studied the interaction of RNA polymerase with rifampicin by use of fluorescence techniques. Addition of saturating concentrations of rifampicin to holo or core enzyme produced a 22% decrease in the tryptophan fluorescence of the enzyme, both in high salt (0.2 M KCl) or low salt (0.05 M KCl) conditions. In the presence of t-RNA or poly U, however, the maximum quenching of the enzyme by rifampicin was reduced to 10%. Fluorescence titration yielded an apparent dissociation constant for the rifampicin-RNA polymerase complex of 4×10^{-9} M which agrees with the K_1 value for rifampicin inhibition (2×10^{-9} M) obtained by steady-state kinetic measurements with T7 DNA as template. Stopped-flow measurements were made of the interaction of core polymerase with rifampicin by monitoring the intrinsic fluorescence of the enzyme. The kinetic data obtained were consistent with a unimolecular isomerization of the enzyme-inhibitor complex subsequent to a bimolecular binding reaction:

$$E + R \underset{k_{-1}}{\overset{k_1}{\rightleftharpoons}} ER \underset{k_{-2}}{\overset{k_2}{\rightleftharpoons}} ER'$$

The best fit value of K_1 (k_{-1}/k_1), the dissociation constant for the binary complex, ER, was 4.1×10^{-5} M. The values for k_2 and k_{-2} were 190 sec^{-1} and 0.005 sec^{-1}, respectively. The overall equilibrium binding constant according to this mechanism was calculated to be 1.1×10^{-9} M from the kinetic constants. Core enzyme reacts at least 10 times more rapidly with rifampicin than does the holo enzyme.

TH-POS-D15 MAGNETIC RESONANCE INVESTIGATION OF THE CONFORMATION OF TRANSFER RNA. W. E. Daniel, Jr.* and M. Cohn, Dept. of Biophysics and Physical Biochemistry, Univ. of Pennsylvania, Philadelphia, Pa. 19174.

A nitroxide spin label has been used to label specifically thiouridine at position-8 in E.coli $tRNA_f^{Met}$ according to Hara et al., BBRC 38, (1970). The rate of the spin-labeling reaction is markedly slowed when divalent metal ions are present. The structure in solution of the spin-labeled-$tRNA_f^{Met}$ has been monitored by EPR in the presence of K^+, NH_4^+, Mg^{++} and spermidine, individually and in various combinations, and compared with the activation of the aminoacylation reaction by these ions. The minimum concentrations of these ions required for folding of the $tRNA_f^{Met}$ correlate well with those needed for the maximal enzyme rates in the charging reaction. In addition, the paramagnetic effect of the nitroxide label on the relaxation times of chemically incorporated fluorine as well as the methyl proton resonances of the odd bases at high field have been examined under conditions where the $tRNA_f^{Met}$ is in the native configuration. In the 220MHz FT-NMR proton spectrum, the ribothymidine methyl resonance was not affected by the spin label while one or both of the superimposed 2'-O-methylcytidine and dihydrouracil resonances and the 7-methylguanine resonance were broadened. Because of the absence of an interaction between the spin label and the ribothymidine methyl group, the distance between the two cannot be calculated. However, we are able to assign a lower limit of 25 Å assuming that a change greater than 10% in T_1 would have been detectable. Similarly the nitroxide spin label had no observable effect on the relaxation time of fluorine incorporated at the -CCA end in the 94 MHz FT-NMR spectrum permitting a lower limit on the spin label to fluorine distance to be determined in that case as well. (Supported by NSF and the American Heart Association, Inc.)

TH-POS-D16 POTENTIAL DISTRIBUTIONS IN PHASE-SEPARATED AQUEOUS POLYMER SOLUTIONS. D.E.Brooks, G.V.F.Seaman, C.H.Tamblyn* and H.Walter, Department of Pathology, Univ.British Columbia, Vancouver, Canada; University of Oregon Medical School, Portland, Ore. and V.A.Hospital, Long Beach, Calif.

Partition in phase separated aqueous solutions of neutral polymers is an extremely sensitive separation technique for cells. In the dextran-polyethylene glycol (PEG) phase system a positive correlation has been found between cell surface charge density and the quantity of cells partitioning into the PEG-rich phase, suggesting electrostatic interactions can determine partition behavior. We have therefore measured electrostatic potential differences between dextran-PEG phases as a function of ionic composition and concentration. We have also measured the partition of the salts themselves in these systems. The potential differences are found to decrease in magnitude the higher the salt concentration and the more disparate the salt partition. Zeta potentials measured at the phase boundary, on the other hand, increase in magnitude with increasing ionic strength and are of opposite sign to those expected from the bulk phase potential differences. The complex potential variation across the phase boundary will be discussed and models considered which might explain such behavior.

TH-POS-D17 TOBACCO MOSAIC VIRUS PROTEIN: KINETIC AND EQUILIBRIUM STUDIES ON THE pH-DEPENDENT TRANSITION A-PROTEIN→DOUBLE DISC.
A. L. Adiarte, D. Vogel* and R. Jaenicke*, Department of Biochemistry, University of Regensburg, 84 Regensburg, Germany.

Stopped flow experiments were performed on TMV-protein under conditions favoring the transition: A-protein → double disc (pH 8→pH 7, 0.1 ionic strength). Concentration dependence studies (1-7 mg/ml) show that above a critical concentration the reaction is described by 3 phases: a rapid biphasic reaction consisting of a nucleation and a propagation step, and a third phase which is tentatively explained as a slow dissociation of higher aggregates into double discs. The order of reaction n is ~3 for both nucleation and propagation and the reaction rate of propagation is greater than that of nucleation. Ultracentrifugal analysis ~10 minutes after mixing shows the presence of higher aggregates (>25 S) which slowly dissociate into double discs and 4-8 S particles, the fraction of the latter being increased with time (>40 hours). Temperature dependence studies (15-25°C) give an activation energy of 4.5 kcal/mole for nucleation; a change in slope of the Arrhenius plot at 21°C is observed for the second phase.

Equilibrium ultracentrifugation shows that the initial and final states correspond to the A-protein and double disc respectively. UV-difference and CD spectra show an increase in UV absorption and a decrease in dichroic absorption at 265 - 290 nm which is caused by tyrosine and/or tryptophan residues. From the time course of the spectral changes, it is concluded that the conformational changes precede the aggregation.

TH-POS-D18 ELECRON DENSITY PROFILE OF NATIVE TENDON COLLAGEN (WET).
R.H. Stinson, J.R. Morrison* and M.W. Bartlett*, Department of Physics, University of Guelph, Guelph, Ontario, Canada.

Small angle X-ray diffraction patterns were obtained from gastrocnemius tendons of 18 day ducklings. Phases were arrived at by subsequent isomorphous replacement (staining) with either phosphotungstic acid or uranyl acetate. Patterson maps of the diffraction patterns of the stained samples and of electron micrographs of the same material permitted the determination of the location of the heavy metal stains and the subsequent phase determination of the various orders of reflection.

TH-POS-D19 EFFECT OF SURFACTANT MICELLES ON THE REMOVAL OF SPIN-LABELED FATTY ACIDS FROM LIPID-PROTEIN COMPLEXES. Wayne W. Sukow[1] and Howard E. Sandberg, Biophysics Program, Wash. State Univ., Pullman, WA. 99163

In a previous report (BBA 298, 209), evidence was presented which linked the protein structural changes observed when membranes are solubilized with anionic surfactants to the transfer of a structure-regulating ligand from the membrane protein to the surfactant micelle. A mechanism for this transfer is studied in a model system. The binding of spin-labeled stearates (SLS) to bovine serum albumin (BSA) provides a lipid-protein system in which the environment of the stearate can be determined. The EPR spectra of the SLS-BSA complex are typical of spherical tumbling, are dependent on the pH-induced conformational changes of BSA, and are dependent on the distance of the doxyl group from the carboxyl group. As the concentration of a nonionic surfactant of the triton X series is increased above the critical micelle concentration (CMC), isoslopic points are dependent on the pH because of the protein conformational dependence. Integration of the EPR spectra results in isosbestic points in the superimposed EPR absorption spectra. The existence of these isosbestic points is taken as evidence for a two state system. Because of the simplicity of the system it is deduced that the SLS are either bound to the BSA or intercalated in the surfactant micelle. Supported by NSFGB-36054. 1) Dept. of Physics, Univ. of Wisc., River Falls, R.F., Wisc.

TH-POS-D20 Determination of A⇌B Transition in DNA by Lasar Raman Spectroscopy - R. Herbeck, S. Mansy and W. L. Peticolas*, Department of Chemistry, University of Oregon, Eugene, Oregon 97403

The A⇌B transition in DNA has been studied by Raman spectroscopy and circular dichroism under a wide variety of conditions -- in oriented crysta-line fibers, in disoriented fibrous masses, in oriented and disoriented gels and in ethanol/water mixtures. Using crystalline fibers we have been able to obtain an exact correlation between the familiar A and B X-ray diffraction patterns and the Raman spectra in the 750-850 cm^{-1} region. We find that at 92% relative humidity the fibers change from the B to the A form only if the fiber is disoriented by dissolving and lypholyzing or if it contains a large amount of added salt. Oriented salt free fibers tend to stay in the A form at high water content including oriented gels (50%). A sharp cooperative change in B→A form occurs in a fiber immersed in EtOH/H_2O solution in going from 70% to 80% EtOH. Cross-linking the DNA with UV radiation locks the DNA in the B form and prevents the transformation to the A form at low water content.

* Supported by NIH grant No. CA03254-01

TH-POS-D21 COMPARISON OF THE GEOMETRY OF NUCLEOSIDE TRIPHOSPHATES ON DNA POLYMERASE AND PYRUVATE KINASE AS DETERMINED BY NMR. D.L. Sloan*, L.A. Loeb, A.S. Mildvan, Institute for Cancer Research, Philadelphia, Pa. 19111

The effects of Mn^{2+} bound at the active site of E. coli DNA polymerase I (EDP) and muscle pyruvate kinase (PK) on the longitudinal ($1/T_{1p}$) and transverse ($1/T_{2p}$) relaxation rates of phosphorus and protons of the enzyme bound nucleotides dTTP and ATP respectively were measured at 40.5, 100 and 220 MHz. The frequency dependence of $1/T_{1p}$ yielded correlation times of 0.9 and 0.8 nsec for the EDP and PK systems respectively. On EDP, proton to Mn^{2+} distances of 10.9, 10.4, 10.8, 11.3 and 8.8 Å for the CH_3-, C_6, C_1', C_2', and C_4' protons of TTP and Mn^{2+} to P distances of 4.5, 5.1, and 3.4 Å for the α,β, and γ phosphorus atoms were calculated, indicating Mn^{2+} coordination of γ only and a puckered triphosphate conformation. On PK, Mn^{2+} to proton distances of 4.7, 7.7 and 9.8 Å were calculated for the C_8, C_2 and C_1' protons of ATP. The Mn^{2+} to P distances (4.6-4.8 Å) indicate a predominantly second sphere complex on PK. The 8 Mn-substrate distances on EDP are fit by a unique Mn-dTTP conformation indistinguishable from that found in double stranded DNA-B. Hence binding to DNA polymerase may adjust the conformation of TTP for Watson-Crick base pairing.

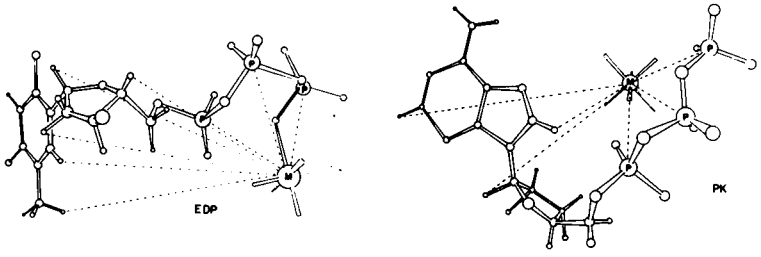

TH-POS-D22 SOLVENT ACCESSIBILITY IN SOYBEAN TRYPSIN INHIBITOR-TRYPSIN COMPLEX FROM HYDROGEN EXCHANGE KINETICS. C.K. Woodward, Dept. of Biochemistry, Univ. of Minnesota, St. Paul, MN 55101.

The hydrogen-tritium exchange kinetics of peptide NH protons in the trypsin-STI complex are markedly slower than the kinetics calculated from the sum of the exchange kinetics for STI and trypsin measured individually at the same pH and temperature. The curved first order plots of the exchange kinetics for the complex are shifted to slower rates compared to the calculated sum of the individually measured STI and trypsin, with a difference of ≈35 protons between the curves. This cannot be accounted for by the formation of either inter- or intramolecular H-bonds. The difference is ascribed to a decrease in solvent accessibility due to an increase in rigidity in the two proteins upon formation of the complex. Since the STI-trypsin complex is dissociated at pH 2, and tightly associated at pH 6.5, experiments can be done to determine whether there is a decrease in solvent accessibility for all exchangable protons, or in only a portion of them. This is done by exchanging equimolar amounts of STI and trypsin at pH 2 for ≈18 hours, then raising the pH to 6.5. Subsequent exchange kinetics of the complex after the pH change are compared to the exchange kinetics at pH 6.5. Our results indicate that the exchange rates of ≈35 peptide NH protons are differentially attenuated by complex formation. Since the contact region of the complex covers a small portion of the component proteins, this indicates that while the solvent accessibility is not decreased uniformly throughout the proteins upon complex formation, decreased solvent accessibility is not limited to the intermolecular contact region

TH-POS-D23 USE OF LANTHANIDE PORPHYRINS AS PARAMAGNETIC PROBES OF HEMOPROTEINS. T. S. Srivastava*, Robert Hershberg* and Takashi Yonetani. Department of Biophysics and Physical Biochemistry, University of Pennsylvania, Philadelphia, Pennsylvania 19174.

Several lanthanide porphyrins have been prepared and their ^1H NMR spectra have shown that they can be used as paramagnetic probes of hemoproteins. They may further find applications as heavy atom probes for X-ray structure determination and electron microscopy. The acetate derivatives of yttrium-(III) mesoporphyrin IX, europium-(III) mesoporphyrin IX, gadolium-(III) mesoporphyrin IX and ytterbium-(III) mesoporphyrin IX have also been prepared. Their incorporation into myoglobin have been achieved by usual method. These are purified by gel filtration. The characterization of these metal-substituted myoglobin complexes have been carried out using visible, electron spin resonance and proton nuclear magnetic resonance spectroscopy. The advantages of ytterbium-substituted myoglobin over iron-(III) substituted myoglobin have been discussed.

Supported by NIH HL-14508 and NSF BMS-73-00970.

TH-POS-D24 A CRYSTALLOGRAPHIC STUDY OF DEOXY COBALT(II)MESOPORPHYRIN IX MYOGLOBIN. E.A. Padlan and W.A. Eaton*, Laboratories of Molecular Biology and Chemical Physics, National Institute of Arthritis, Metabolism and Digestive Diseases, National Institutes of Health, Bethesda, MD 20014, and T. Yonetani, Johnson Research Foundation and Department of Biophysics and Physical Biochemistry, University of Pennsylvania School of Medicine, Philadelphia, PA 19174.

The crystal structures of acid metmyoglobin and deoxy cobalt(II)mesoporphyrin IX myoglobin are compared by a difference Fourier analysis at 2.5 A resolution. No large differences in protein conformation are observed. The greatest density of structural differences is found in the heme region. There is a loss of the histidine-bound sulfate ion and of the metal-bound water molecule, as well as a shift in the position of the prosthetic group with associated changes in the adjacent globin. The structural changes resulting from the substitution of ethyl for the vinyl side chains of the porphyrin are clearly observed. There is also a suggestion of a conformational change of the porphyrin ring. It is not clear whether there is any change of the metal position relative to the porphyrin plane or proximal histidine.

TH-POS-D25 CHARACTERIZATION OF THE SECONDARY STRUCTURE OF HUMAN FACTOR XI (PLASMA THROMBOPLASTIN ANTECEDENT). by C. R. McMillin, A. G. Walton, H. Saito* and O. Ratnoff*, Department of Macromolecular Science, Case Western Reserve University, Cleveland, Ohio 44106.

Plasma throboplastin antecedent (PTA, factor XI) is a plasma protein participating in the early stages of surface-activated blood coagulation. Amino acid analysis of purified human PTA and results of a conformational study of this protein using circular dichroism spectroscopy are reported. Analysis of the amino acid residue content of PTA by the method of Kotelchuck and Scheraga showed that 28% of the residues were α-helix formers, 40% were α-helix disruptors, and the rest were indifferent. The circular dichroism spectrum of PTA suggests that the main conformation present is the β-sheet conformation. This structure was fairly stable when perturbed with solvents, pH, adsorption to dry quartz surfaces and temperature, but when changes occurred, they were rapid and irreversible. The PTA aggregated in the presence of small amounts of NaCl at approximately 70°C upon heating. In the absence of NaCl, the 217 nm band, indicative of β-sheet conformation, increased in intensity between 60°C and 85°C, in an irreversible manner. Trypsin-activated PTA had the same conformation and the same type of heat denaturation curve as unactivated PTA, as determined by CD spectroscopy. Thus, no gross changes occur in the secondary structure of the PTA molecule when it is activated by trypsin. This work was supported in part by USPHS under grant number HL-02783-01.

TH-POS-D26 MAGNETIC CIRCULAR DICHROISM EVIDENCE FOR LOW SPIN FERROUS HEME IN NON-COOPERATIVE DEOXY HEMOGLOBINS. Larry Vickery, Rukmani Pennathur, Mary L. Adams* and Todd M. Schuster, Laboratory of Chemical Biodynamics, University of California, Berkeley 94720, and Biological Sciences Group, University of Connecticut, Storrs 06268.

Magnetic circular dichroism (MCD) spectra at 4°, pH 7, of deoxy isolated α and β subunits (-SH regenerated) of human hemoglobin A_0 (Hb-A) exhibit Faraday A terms at 571 and 572 nm, respectively, which are not present in deoxy tetrameric Hb-A. A similarly shaped MCD band is also found in stripped deoxy hemoglobin Kempsey (Hb-K), $\alpha_2^A\beta_2^{99}$ asp→asn), kindly supplied by Dr. H. F. Bunn. Addition of inositol hexaphosphate (IHP), which increases the Hill coefficient of Hb-K from 1.1 to 1.7, causes a decrease in the intensity of this A type band. The shape of the MCD difference spectrum of Hb-K (-IHP vs. +IHP), with a zerocrossing at 572 nm, is typical of a low spin reduced heme but does not resemble any high spin complexes; it is also distinct from the MCD of oxy Hb-A (A band at 575 nm) and a Hb hemochrome in which the distal histidine is coordinated to the iron (A band at 559 nm). Thus while Hb-A appears to be completely high spin (S=2), the non-cooperative forms studied have a detectable fraction of the heme in the low spin (S=0) state. By analogy with model heme compounds in which changes in spin state of the iron are coupled to its position relative to the porphyrin plane, a shift toward low spin in non-cooperative forms may reflect a relaxation of conformational restraints which hold the iron out of the porphyrin plane and maintain the completely high spin state in Hb-A (see for example Perutz et al., Biochemistry 13, 2187, 1974).

[Supported in part by the USAEC and USPHS Grants GM-18472 and AI-11573]